

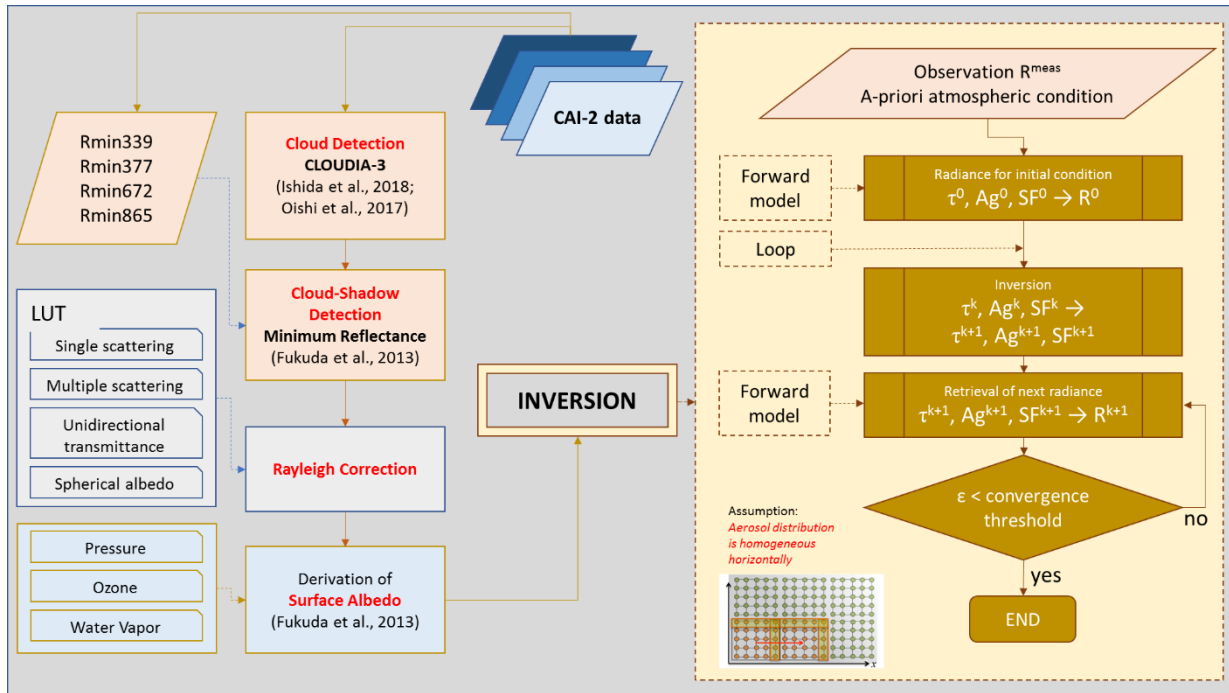
Supplementary Materials

Table T1: Network of aerosol observatories in the ARFINET and their regional classification.

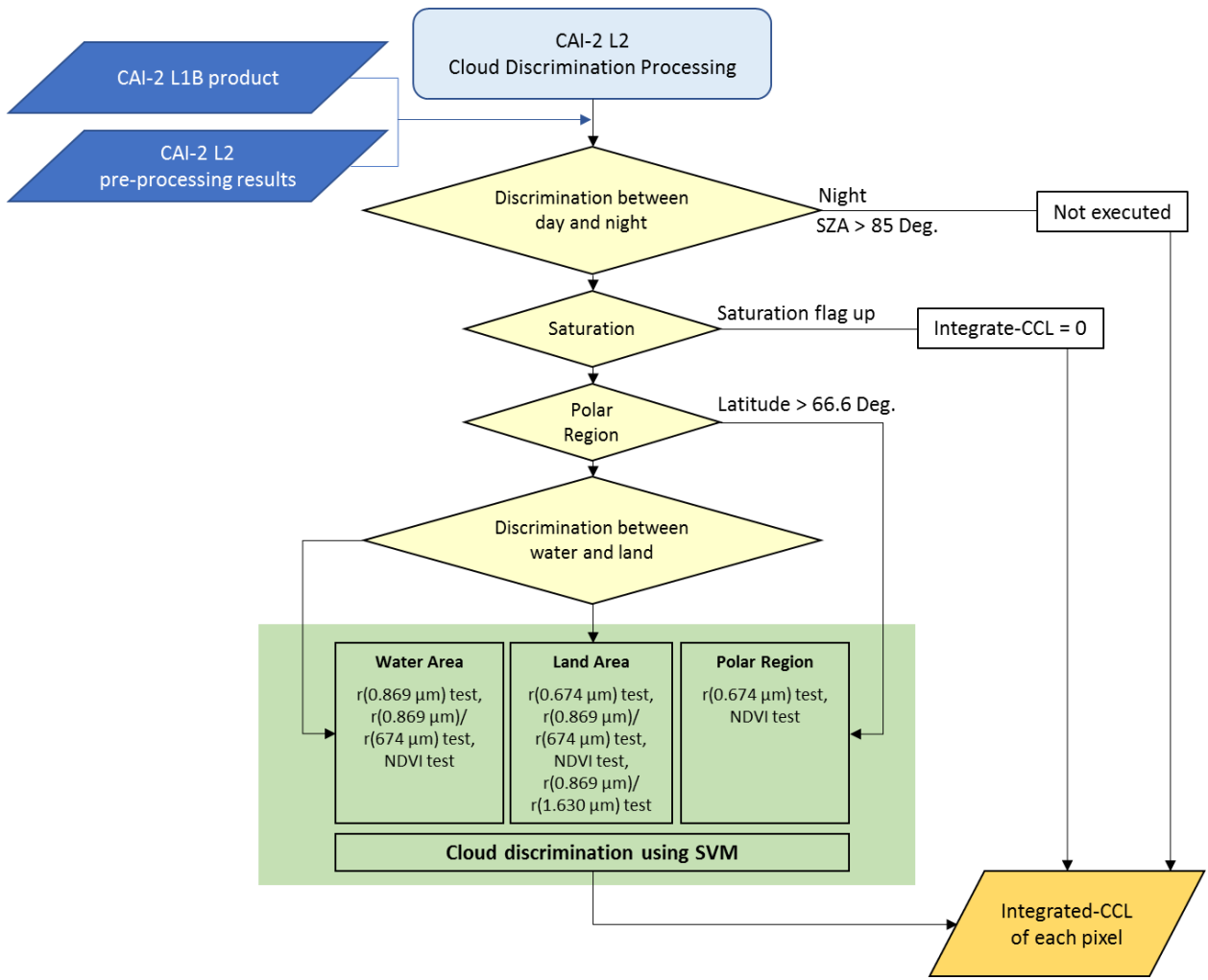
Region	Station Name	Station Code	Latitude	Longitude
IGP – Indo Gangetic Plains	Agra	AGR	27.18	78.02
	Delhi	DEL	28.6	77.2
	Gorakhpur	GKP	26.75	83.38
	Kanpur	KNP	26.4	80.3
	Patiala	PTL	30.33	76.46
	Ranchi	RNC	23.23	85.23
	Varanasi	VNS	25.3	82.96
NEI – North-Eastern India	Agartala	AGT	23.5	91.25
	Dibrugarh	DBR	27.3	94.6
	Imphal	IPH	24.75	93.92
	Kharagpur	KGP	22.5	87.5
	Kolkata	KKT	22.57	88.37
	Shillong	SHN	25.6	91.91
NWI – North-Western India	Ahmedabad	AHM	23.1	72.6
	Jaisalmer	JSL	26.92	70.95
	Naliya	NAL	22.23	68.69
	Rajkot	RJK	22.3	70.73
	Udaipur	UDP	24.6	73.9
HIM – Himalayan, sub-Himalayan and foot-hills of Himalayas	Dehradun	DDN	30.34	78.04
	Hanle	HNL	32.78	78.95
	Kullu	KLU	31.9	77.1
	Lachung	LCN	27.4	88.74
	Nainital	NTL	29.2	79.3
	Tawang	TWG	27.59	91.87
CI – Central India	Nagpur	NGP	21.15	79.15
	Bhubaneshwar	BBR	20.2	85.8
PI – Peninsular India	Anantapur	ATP	14.46	77.67
	Bangalore	BLR	12.97	77.59
	Challakere	CHK	14.32	76.65
	Chennai	CHN	12.7	79.92
	Goa	GOA	15.46	73.83
	Hyderabad	HYD	17.47	78.58
	Kadappa	KDP	14.46	78.81
	Ooty	OTY	11.4	76.7
	Ponmudi	PMD	8.8	77.1
	Pune	PUN	18.54	73.85
	Thiruvananthapuram	TVM	8.5	77
	Vijayawada	VJD	16.44	80.62
	Visakhapatnam	VSK	17.7	83.1
IL – Island Location	Port-Blair	PBR	11.64	92.71

5 **Table T2: Statistical fit parameters between satellite-retrieved (BC_{SAT} , 1 x 1-degree horizontal grid) and near-surface BC (BC_{SUR} , climatological monthly average values at different stations during 13:00 – 14:00 hrs. local time for the period 2015-2019) concentrations at different months.**

	R	slope	intercept	N
Dec	0.36	0.39 ± 0.22	2.36 ± 0.64	25
Jan	0.46	1.23 ± 0.53	0.49 ± 1.25	23
Feb	0.68	0.98 ± 0.21	-0.43 ± 0.61	28
Mar	0.74	1.31 ± 0.23	-0.97 ± 0.62	29
Apr	0.61	1.17 ± 0.30	-0.97 ± 0.76	29
May	0.79	0.66 ± 0.12	-0.04 ± 0.21	26
Jun	0.60	1.12 ± 0.34	0.22 ± 0.41	26
Jul	0.63	3.02 ± 0.77	0.29 ± 0.92	27
Aug	0.60	2.13 ± 0.63	1.22 ± 0.68	24

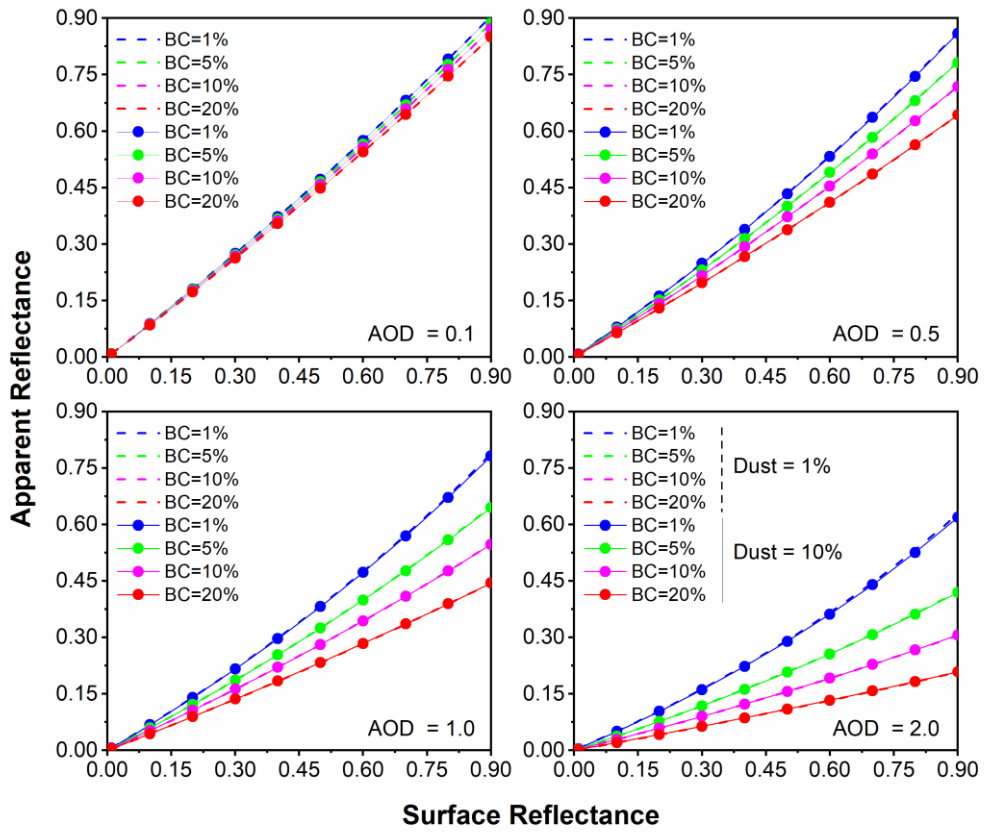


15 Figure S1: Flowchart of CAI-2 L2 pre-processing algorithm (GOSAT-2 project: GOSAT-2/CAI-2 Level-2 Preprocessing Theoretical Basis Document - ATBD).



20

Figure-S2: The Flowchart of flow-chart of the Cloud and Aerosol Unbiased Decision Intellectual Algorithm (CLAUDIA3).



25 **Figure-S3:** Variability of apparent reflectance of satellite observation at 0.880 μm wavelength with surface reflectance for different fractions of BC (1%, 5%, 10% and 20%), dust (1% and 10%) under different conditions of AOD (0.1, 0.5, 1.0, 2.0). The fraction of water-soluble species is kept constant (50%). The solar zenith and azimuth angles are 40° and 100° , and satellite viewing angle and azimuth angle are 45° and 50° respectively. The surface reflectance is considered for homogeneous Lambertian surface.

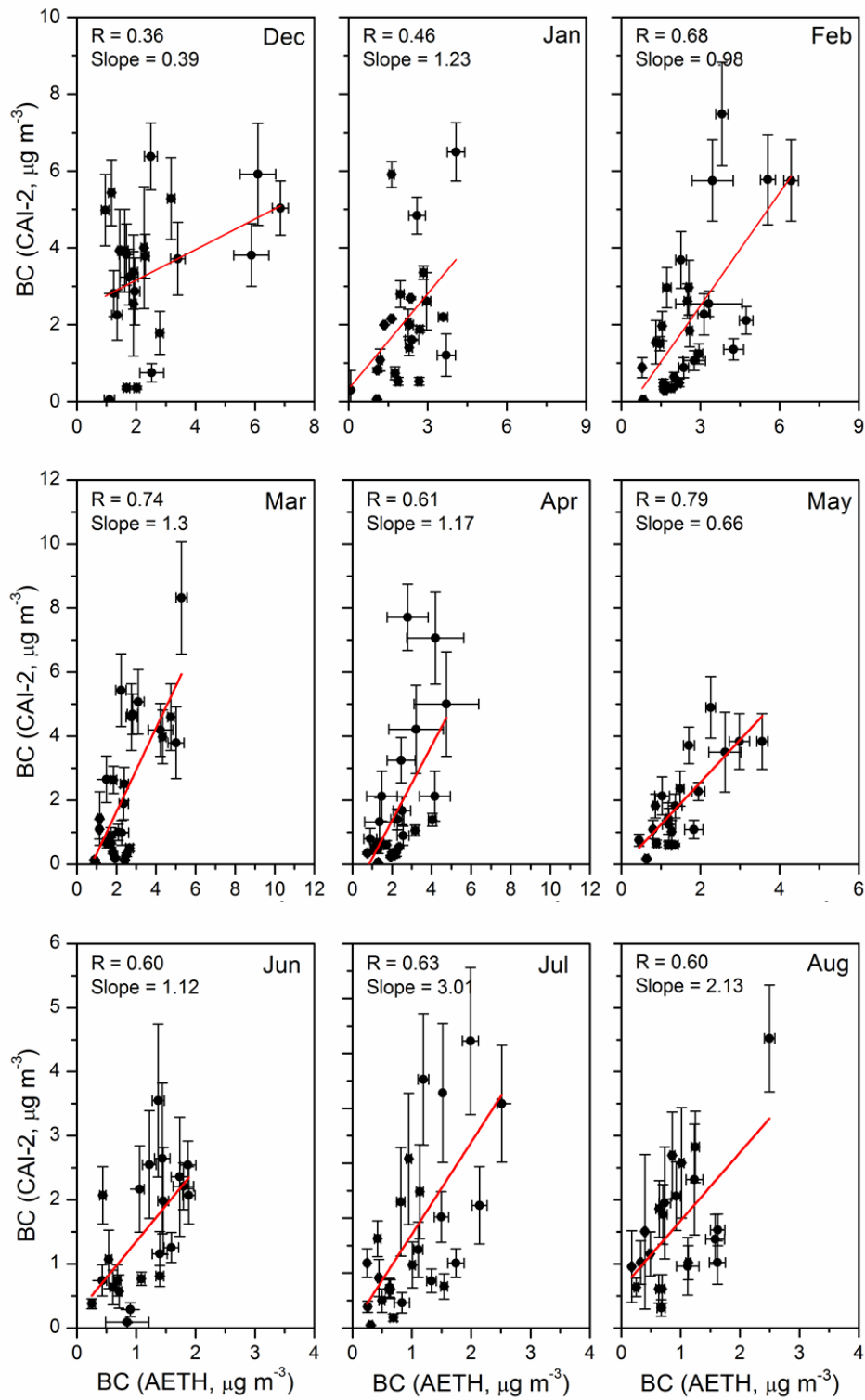
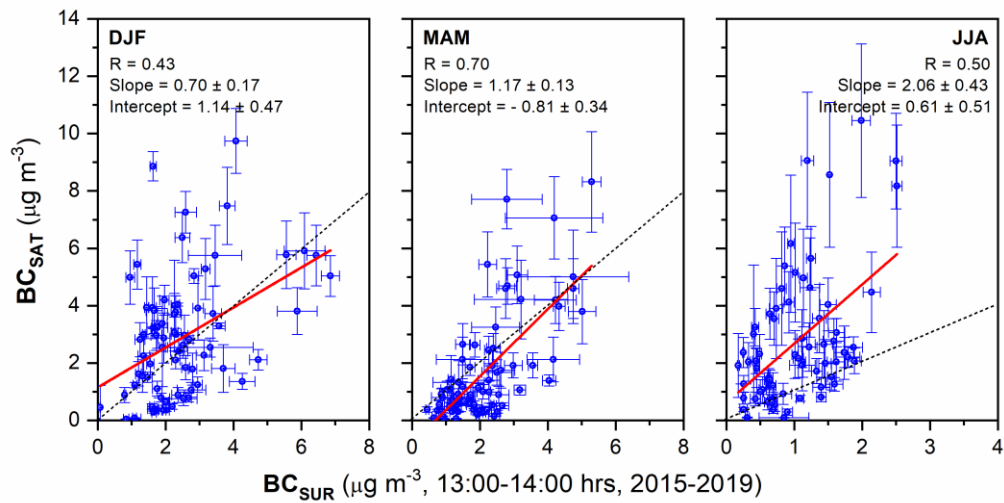


Figure S4: Comparison of monthly average BC from satellite (averaged over 1 x 1-degree area around each of the ARFINET sites) and surface measurements (during 13:00-14:00 hrs. local time for the period 2015-2019) at different locations during DJF, MAM and JJA. The solid red line is the linear fit of BC_{SAT} and BC_{SUR} .

35



40 **Figure S5: Comparison of monthly average satellite BC (1 x 1-degree area average values around each of the point locations in the ARFINET) with surface BC (during 13:00-14:00 hrs. local time for the period 2015-2019) at different seasons, representing winter, pre-monsoon and monsoon. The solid red line is the linear fit, and the grey dash line is the one-to-one line of BC_{SAT} and BC_{SUR} .**

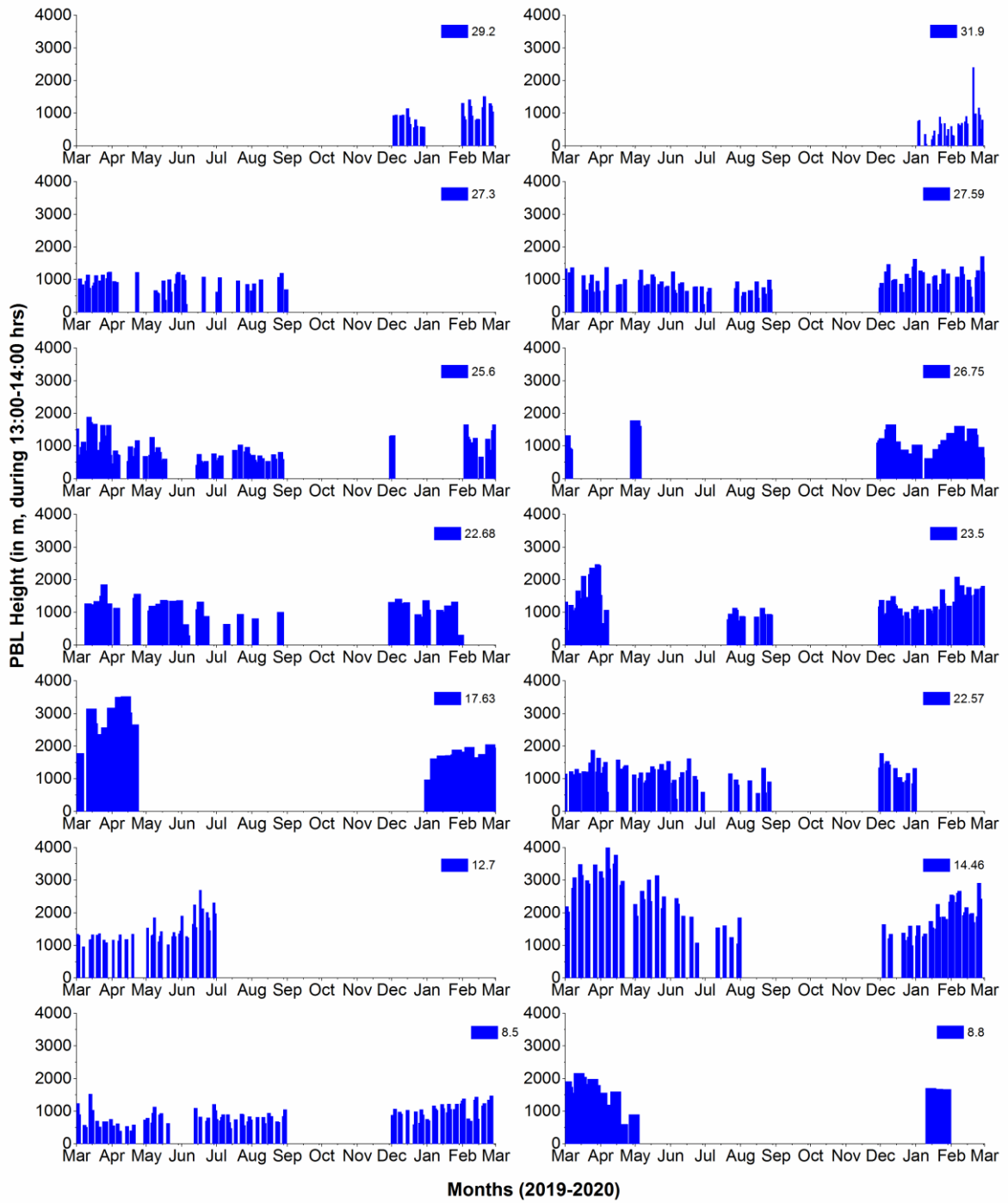


Figure S6: Day to day variability of planetary boundary layer (PBL) height (in m) over different locations of India. The days shown here correspond to the days of simultaneous measurements of BC from satellite and surface.

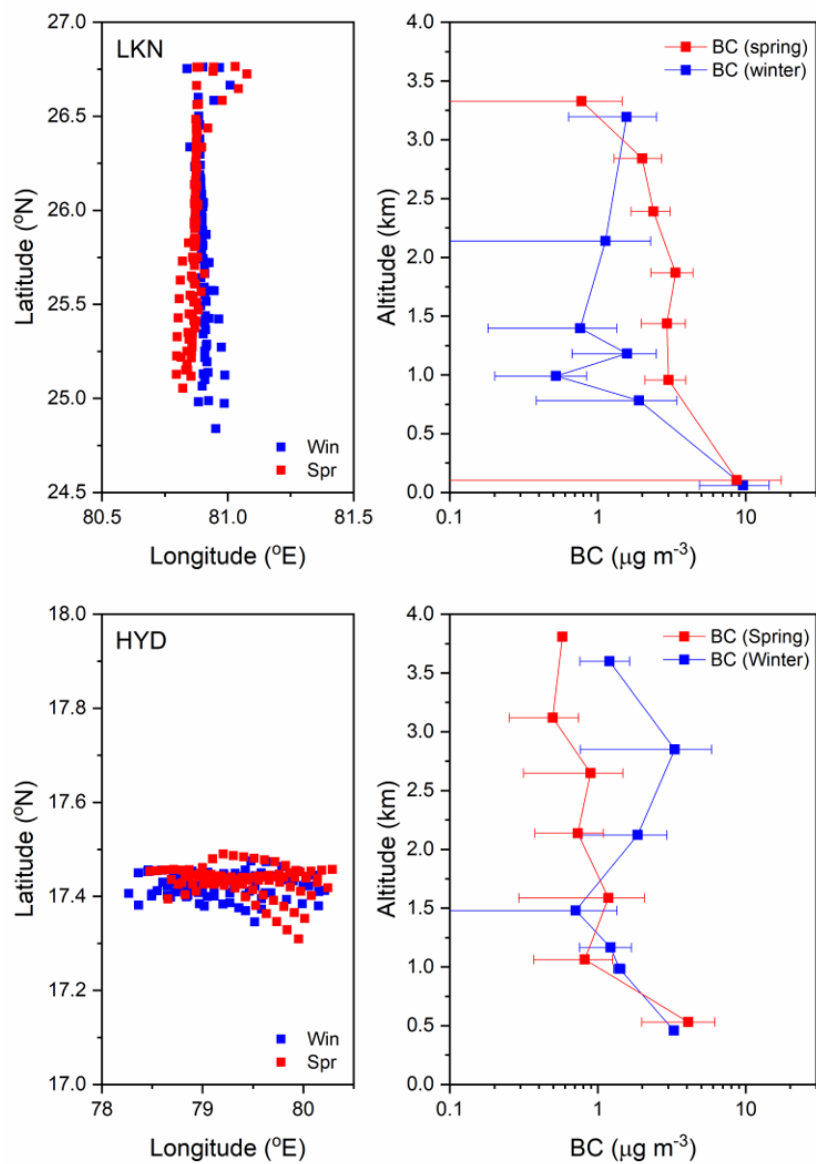


Figure-S7: Vertical profiles of BC (right panels) during two distinct periods of winter (December) and spring (May) over Hyderabad (central India) and Lucknow (Indo-Gangetic Plains). The horizontal bars show the standard deviations of the mean. The foot prints of the data acquisition along the flight tracks are also shown in the left panels.

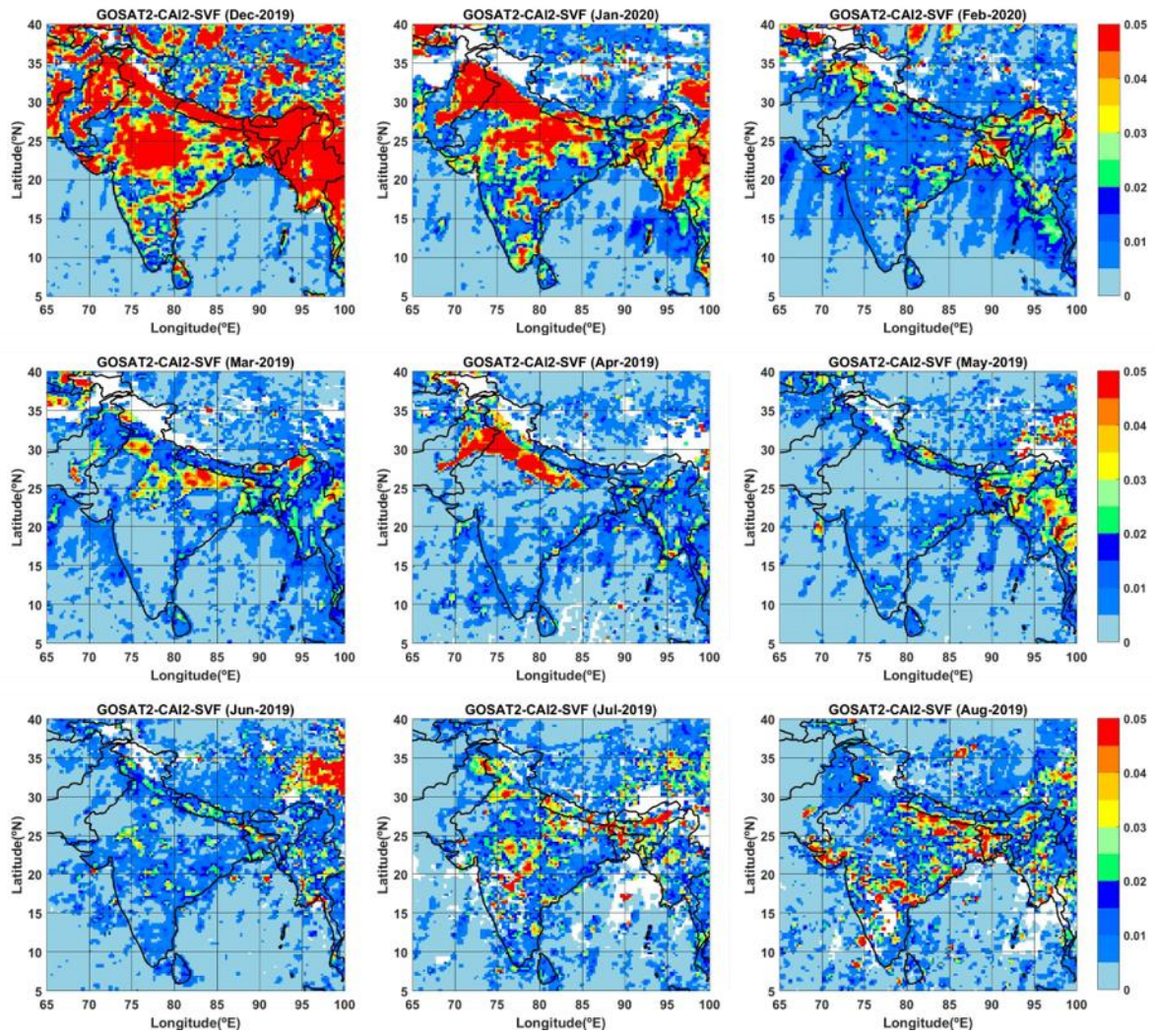
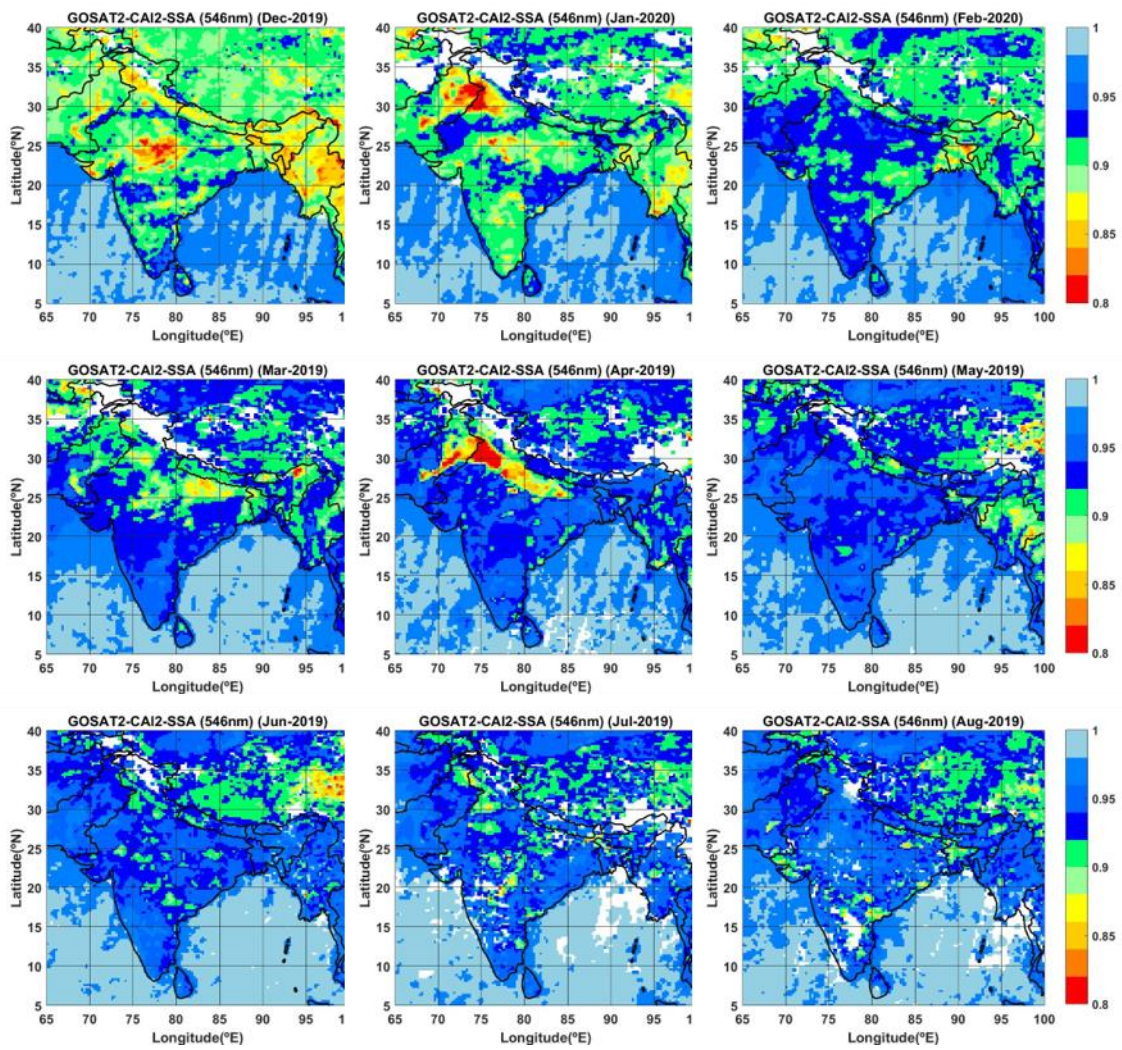


Figure S8: Regional distribution (monthly average) of soot volume fraction (SVF) during DJF, MAM and JJA.



60 Figure S9: Regional map (monthly average) of aerosol single scattering albedo (SSA) at 546 nm during DJF, JJA and MAM from CAI-2.

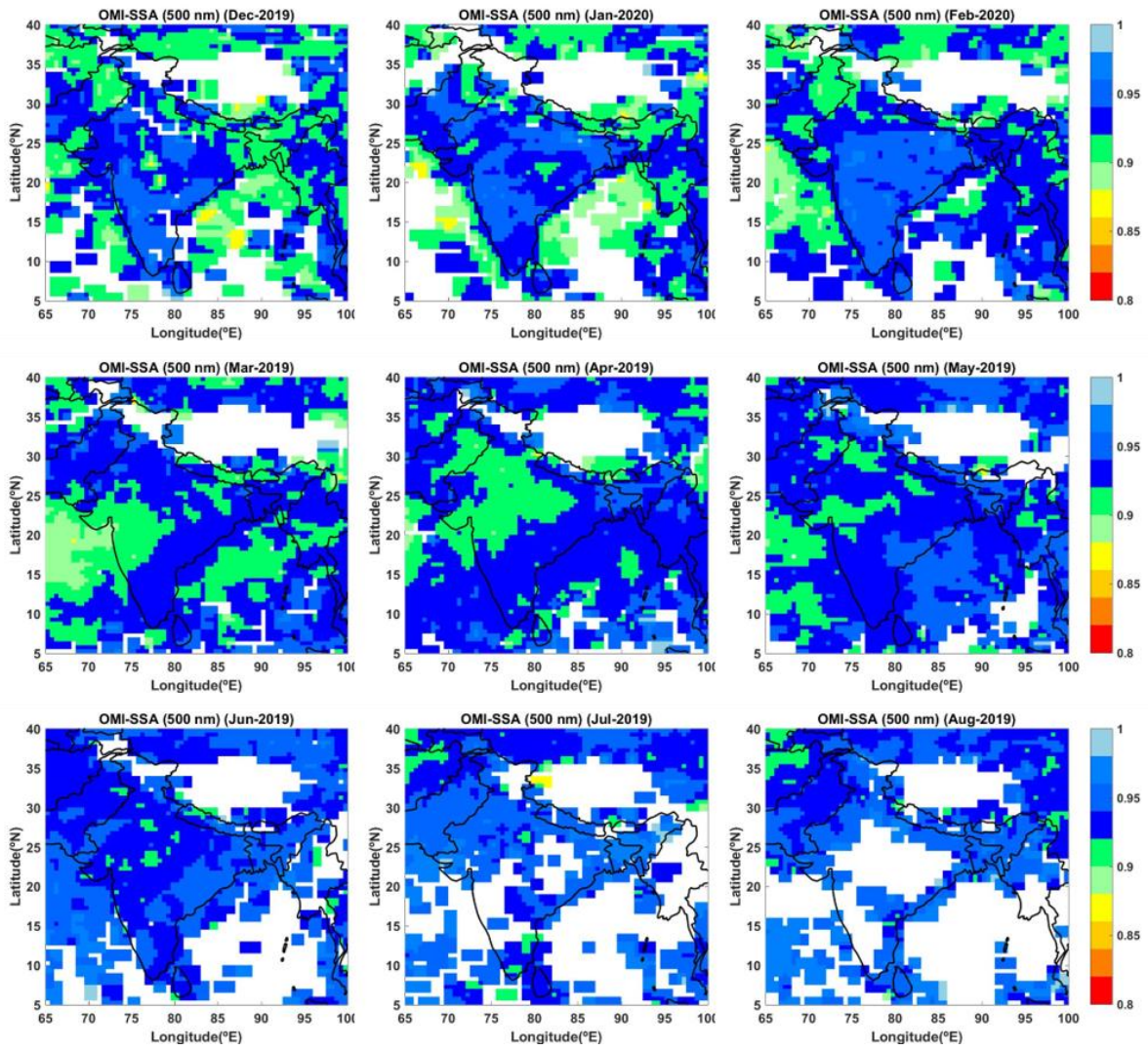


Fig.S10: Regional map (monthly average) of aerosol single scattering albedo (SSA) at 550 nm during DJF, JJA and MAM from 65 OMEAUvd.

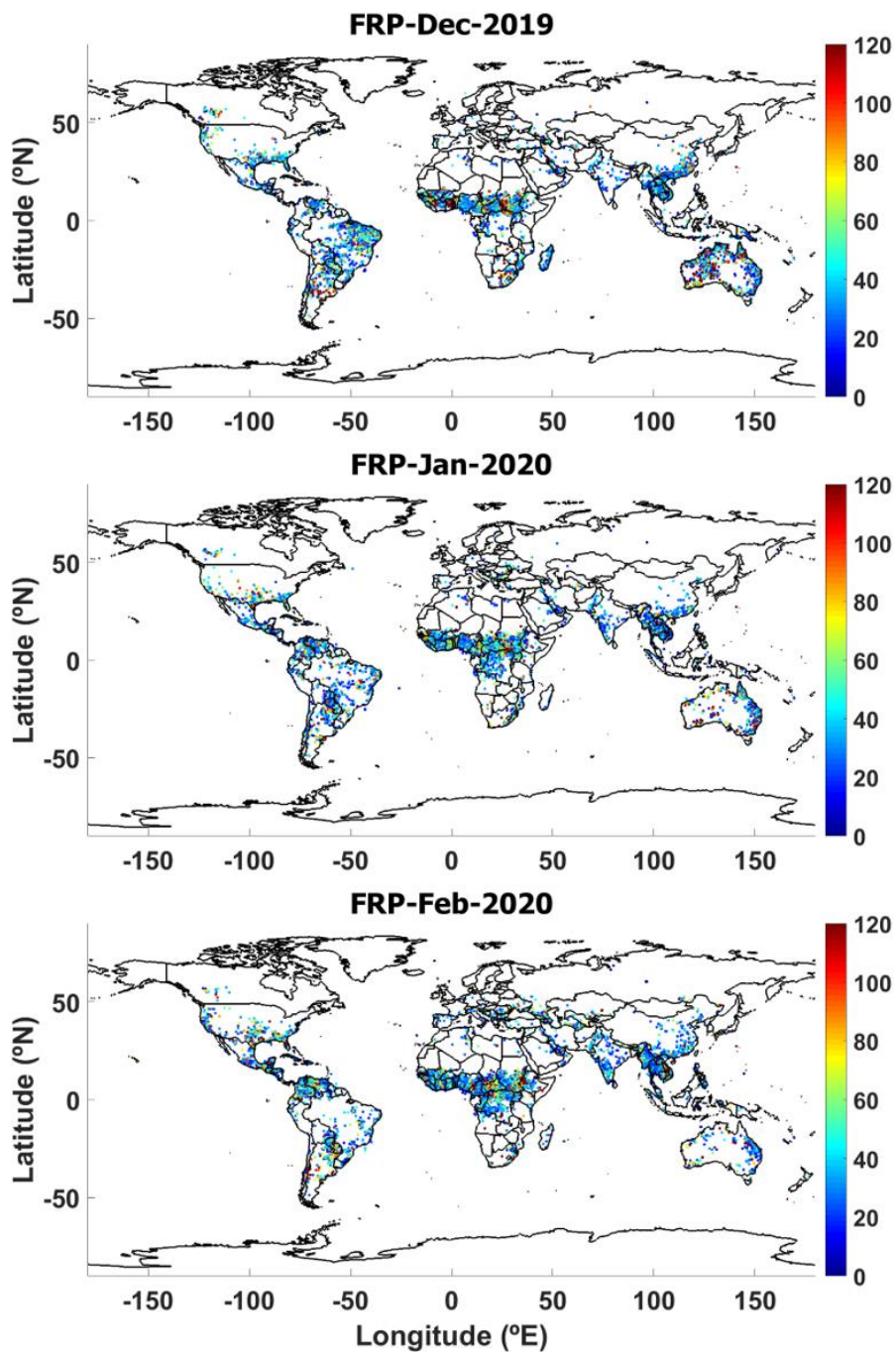
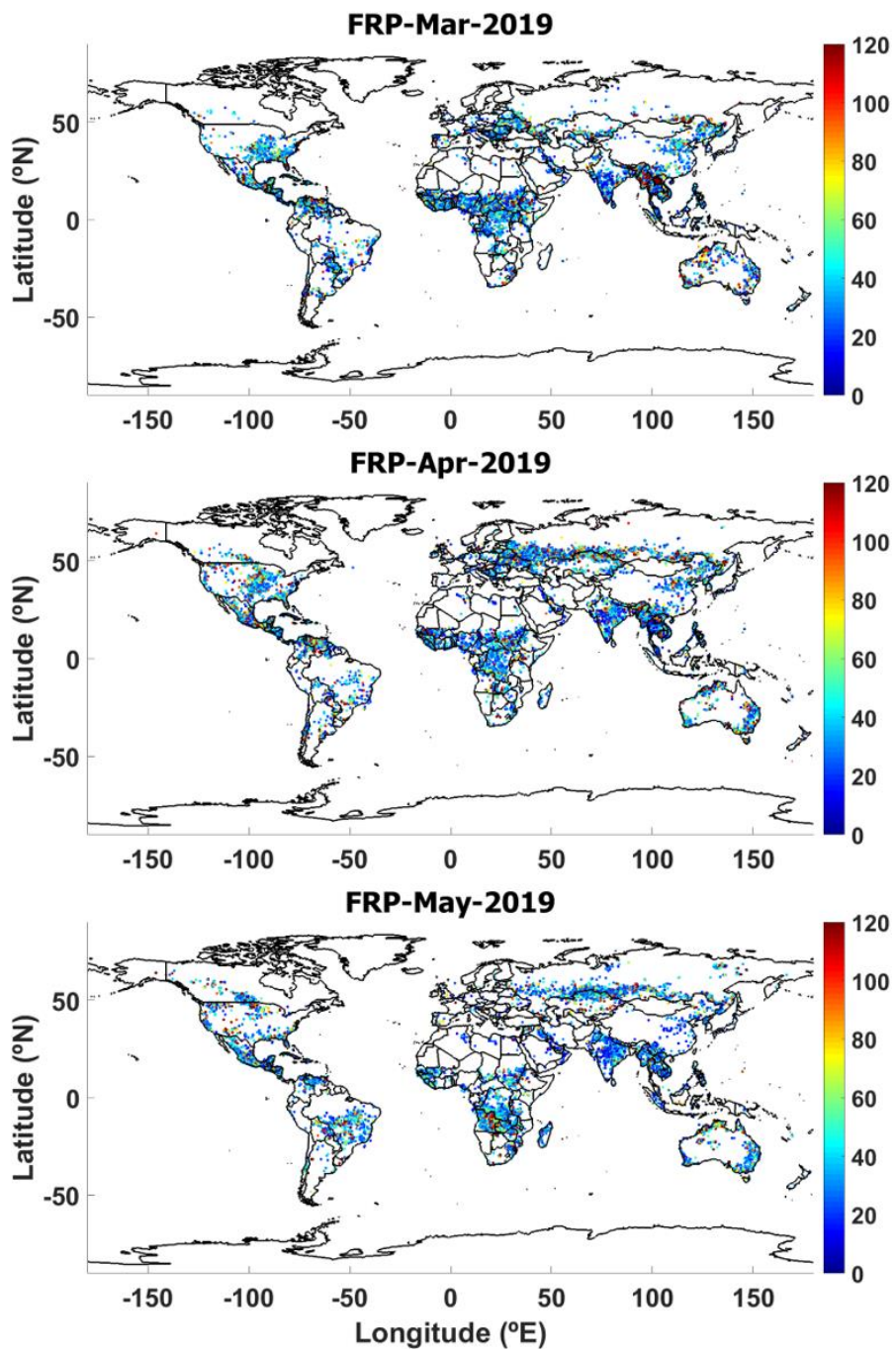


Figure S11: Fire radiative power (FRP, in MW) during DJF.



75

Figure S12: Fire radiative power (FRP, in MW) during MAM.

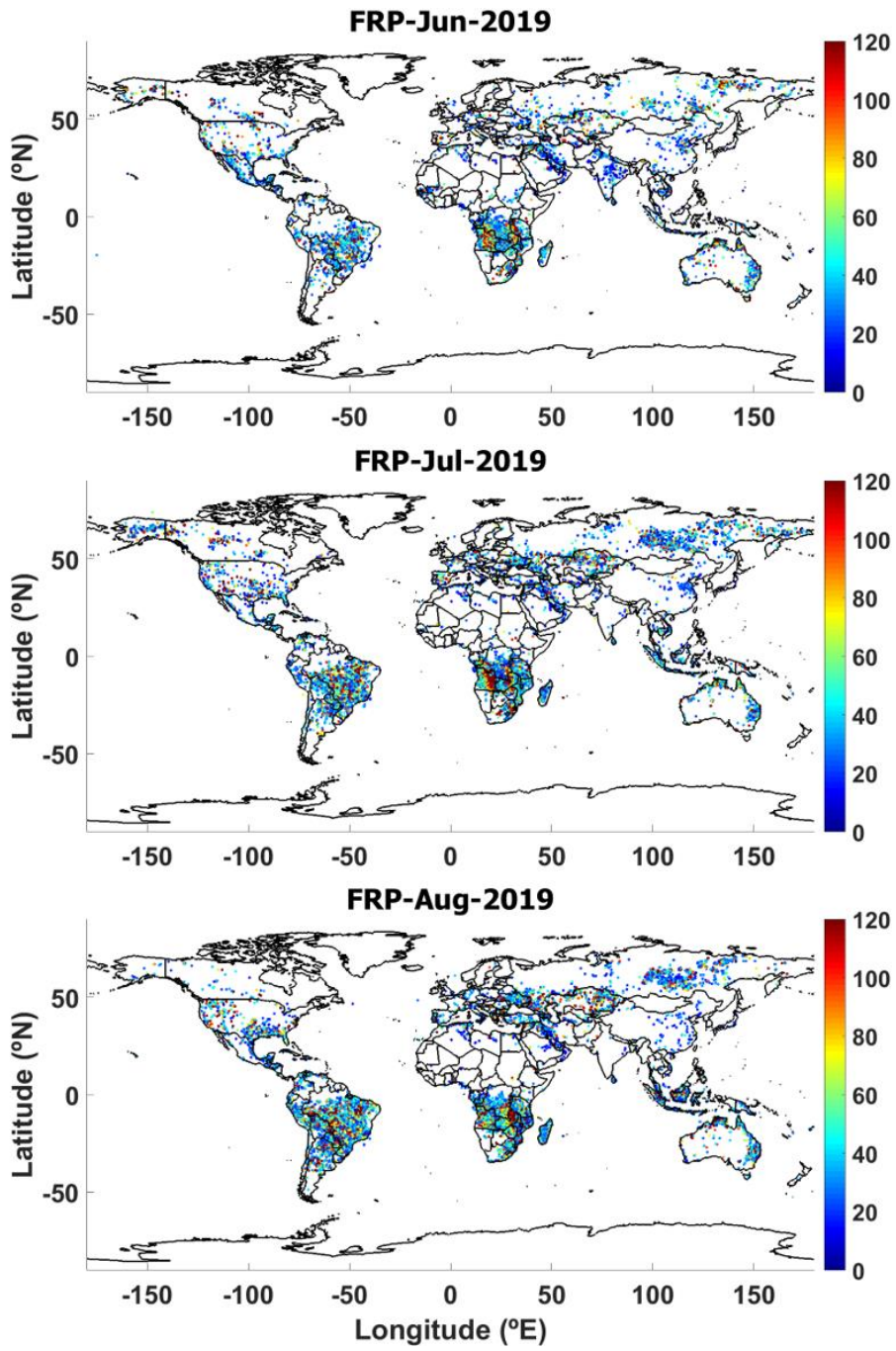
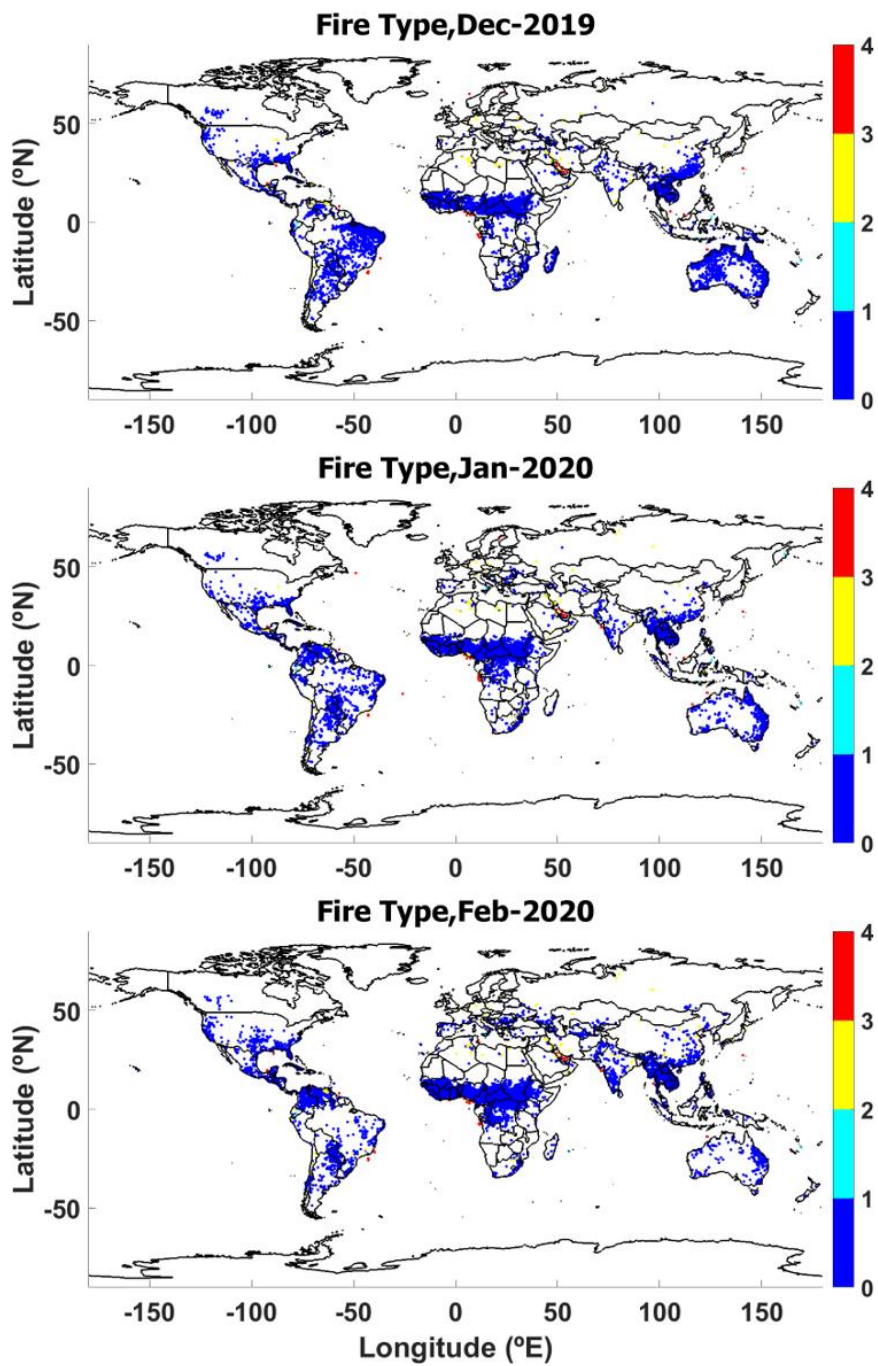


Figure S13: Fire radiative power (FRP, in MW) during JJA.



80

Figure S14: Fire type during DJF; 1 - vegetation fire, 2 - active volcano, 3 - static land shore and 4 - offshore.

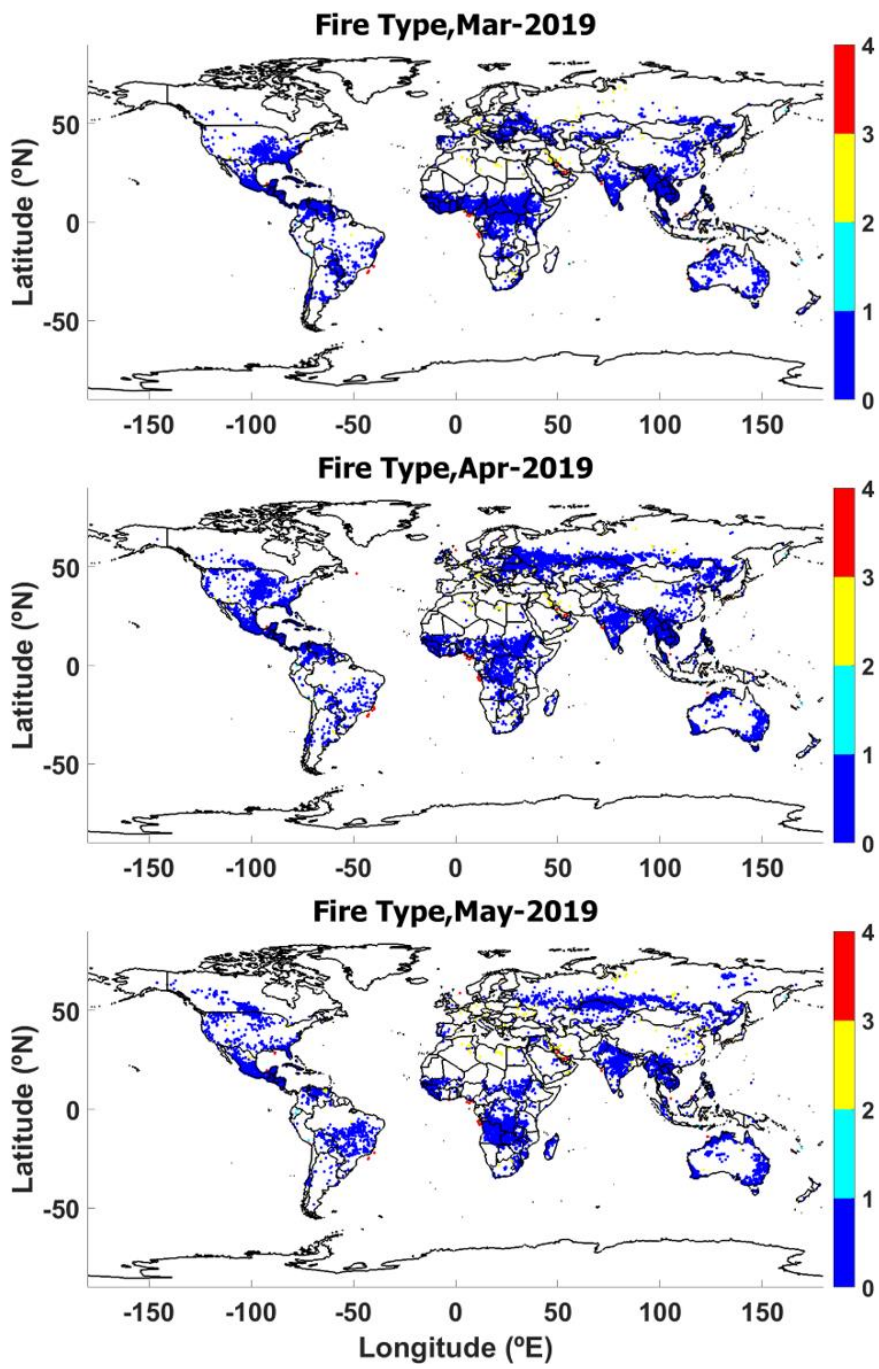


Figure S15: Fire type during MAM.

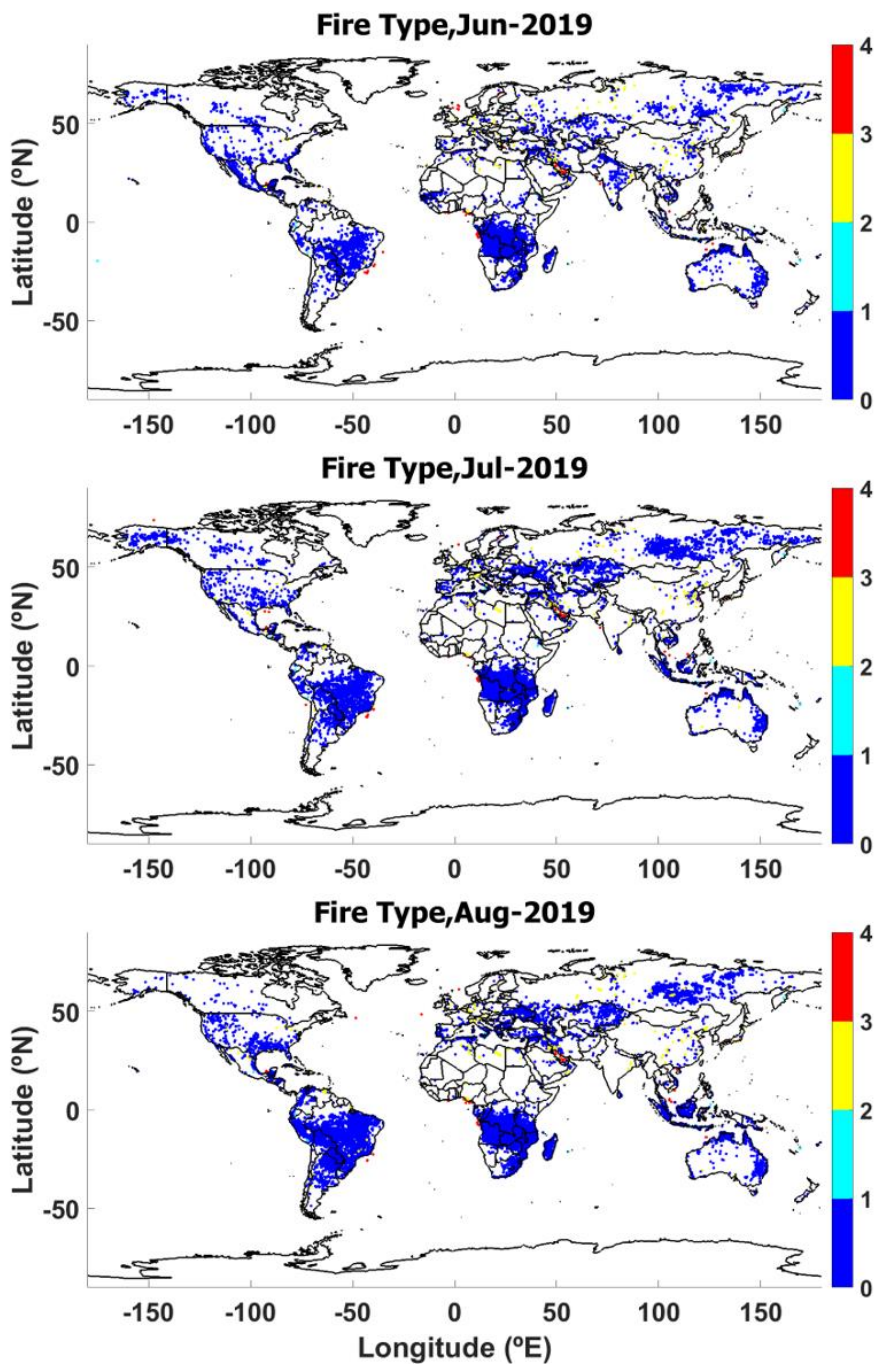


Figure S16: Fire type during JJA.